

waveguides in a plane, we reduce the coupling between each other. The results obtained let us consider different possibilities using this architecture to perform planar antennas with specific features.

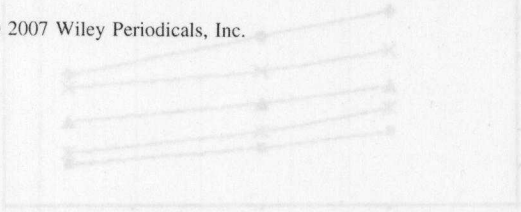
ACKNOWLEDGMENTS

This research work is being supported by a Spanish Government Grant (FPU) and by the Spanish Ministry of Science and Technology under Grant AIMS (TEC2005-05310/TCM). The simulations presented in this work have been realized using CST Microwave Studio Suite 2006 under a cooperation agreement between Computer Simulation Technology (CST) and Technical University of Madrid. NY substrate used in the prototypes was kindly given by NELTEC S.A.

REFERENCES

1. C. Caloz and T. Itoh, *Electromagnetic metamaterials: Transmission line theory and microwave applications*, Wiley, IEEE Press, 2006.
2. D. Sievenpiper, *High-impedance electromagnetic surfaces*, Ph.D. Dissertation, University of California, Los Angeles, 1999.
3. K.P. Ma, K. Hirose, F.R. Yang, Y. Qian, and T. Itoh, Realization of magnetic conducting surface using novel photonic bandgap structure, *IEEE Electron Lett* 34 (1998), 2041-2042.
4. F.R. Yang, K.P. Ma, Y. Qian, and T. Itoh, A uniplanar compact photonic bandgap (UC-PBG) structure and its application for microwave circuits, *IEEE Trans Microwave Theory Tech* 47 (1999), 1509-1514.
5. D.F. Sievenpiper, L. Zhang, R.F. Broas, N.G. Alexopoulos, and E. Yablonovitch, A high-impedance electromagnetic surfaces with forbidden frequency band, *IEEE Trans Microwave Theory Tech* 47 (1999), 2059-2074.
6. J.M. Fernández and M. Sierra-Castañer, Electromagnetic bandgap structures as artificial magnetic conductor surfaces sidewalls in parallel plate slot antennas, *Microwave Opt Technol Lett* 48 (2006), 1441-1446.
7. R.S. Elliott, On the theory of corrugated plane surfaces, *IRE Trans Antennas Propag AP-2* (1954), 71-81.
8. R.E. Collin, *Field theory of guided waves*, 2nd ed., New York, IEEE Press, 1991.
9. K.W. Whites, B. Glover, and T. Amert, Easily designed and constructed high impedance surfaces, 2003 IEEE AP-S International Symposium on Antennas and Propagation, Columbus (Ohio), *IEEE Antennas Propag Soc Int Symp Dig*, 2 (2003), 407-410.
10. F.R. Yang, K.P. Ma, Y. Qian, and T. Itoh, A novel TEM waveguide using uniplanar compact photonic bandgap (UC-PBG) structure, *IEEE Trans Microwave Theory Tech* 47 (1999), 2092-2098.
11. P.-S. Kildal, Definition of artificially soft and hard surfaces for electromagnetic waves, *Electron Lett* 24 (1988), 168-170.
12. P.-S. Kildal, Artificially soft and hard surfaces in electromagnetics, *IEEE Trans Antennas Propag* 38 (1990), 1537-1544.
13. J.A. Aas, Properties of waves guided between parallel, artificially hard surfaces, *IEEE Antennas Propag Soc Int Symp Dig* 1 (1993), 390-393.
14. M. Sierra-Castañer, J. Izquierdo, M. Sierra-Pérez, J.L. Fernández-Jambrina, and M. Vera-Isasa, Linear polarization parallel plate slot antenna, *IEEE AP-S Symp* 3 (2000), 1608-1611.
15. H. Kai, J. Hirokawa, and M. Ando, Analysis of inner fields and aperture illumination of an oversized rectangular slotted waveguide, *IEEE Proc Microwave Antennas Propag* 150 (2003), 415-421.

© 2007 Wiley Periodicals, Inc.



COMPARISON OF MICROWAVE AND ELECTRICAL PROPERTIES OF SELECTED CONDUCTING POLYMERS

K. Lakshmi,¹ Honey John,² Rani Joseph,² K.E. George,² and K.T. Mathew³

¹ Department of Polymer Engineering, Amrita University, Coimbatore 641105

² Department of Polymer Science and Rubber Technology, Cochin University of Science and Technology, Kochi 682022

³ Department of Electronics, Cochin University of Science and Technology, Kochi 682022; Corresponding author: ktm@cusat.ac.in

Received 21 June 2007

ABSTRACT: Microwave properties of conductive polymers is crucial because of their wide areas of applications such as coating in reflector antennas, coating in electronic equipments, frequency selective surfaces, EMI materials, satellite communication links, microchip antennas, and medical applications. This work involves a comparative study of dielectric properties of selected conducting polymers such as polyaniline, poly(3,4-ethylenedioxythiophene), polythiophene, polypyrrole, and poly(paraphenylene diazomethine (PPDA) in microwave and DC fields. The microwave properties such as dielectric constant, dielectric loss, absorption coefficient, heating coefficient, skin depth, and conductivity in the microwave frequency (S band), and DC fields were compared. PEDOT and polyaniline were found to exhibit excellent properties in DC field and microwave frequencies, which make them potential materials in many of the aforementioned applications. © 2007 Wiley Periodicals, Inc. *Microwave Opt Technol Lett* 50: 504–508, 2008; Published online in Wiley InterScience (www.interscience.wiley.com). DOI 10.1002/mop.23091

Key words: conducting polymers; microwave properties; cavity perturbation technique

1. INTRODUCTION

Intrinsically conducting polymers are usually extensively conjugated molecules. Conjugated polymers are—in their pristine, neutral state—either insulators or wide-gap semiconductors, and some of them turn into metallic type conductors after a process called doping. Conducting polymers having π -electron conjugated structure, such as polyacetylene, polyaniline, polypyrrole, polythiophene (PTH), polyfuran (PFU), poly(para phenylene vinylene), and polycarbazole have been synthesized for exploring them in many applications [1]. The intrinsically conducting polymers have many physically and chemically desirable features such as lightweight, processability, structure modification, and electrical conductivity, and, therefore, potential application as microwave active materials [2]. Microwave properties of conductive polymers is crucial because of their wide areas of applications such as coating in reflector antennas, coating in electronic equipments, frequency selective surfaces, EMI materials, satellite communication links, microchip antennas, radar, and microwave absorbing materials [3-5]. Nonbiological materials exhibiting the dielectric properties of biological tissue at microwave frequencies have been used extensively to evaluate hyperthermia applicators, assess microwave imaging systems, and determine electromagnetic absorption patterns, among other applications [6, 7].

A conductive plastic composite that exhibits complex dielectric properties similar to biological tissues over the electromagnetic spectrum of 300–900 MHz has been synthesized from compressed carbon black mixed with a castable thermoplastic [8]. A solid-gel muscle phantom made of polyacrylamide (PAG) was developed for use in the short-wave frequency range (13–40 MHz) and was later adapted for microwave applications by Andreuccetti et al. [9].

2. EXPERIMENTAL

2.1. Preparation of Conducting Polymers

PTH was prepared by chemical oxidative polymerization of thiophene in nitrobenzene solvent using anhydrous ferric chloride (FeCl_3) as oxidant [10]. The polymer was then doped in 1 M FeCl_3 solution in nitromethane for 24 h. Poly (3,4-ethylenedioxythiophene)-PEDOT was prepared in aqueous dodecyl benzene sulfonic acid (DBSA) micellar solution using FeCl_3 as oxidizing agent [11]. Chemical oxidative polymerization of aniline was carried out in aqueous FeCl_3 solution to get polyaniline [12]. Polyaniline (PANI) was doped with 1 M solution of camphor sulphonic acid for 24 h. Polypyrrole was prepared by the polymerization of pyrrole with ferric chloride in methanol solvent [13]. The polymer was then doped with 1 M FeCl_3 solution in nitromethane for 24 h. Polyparaphenylene diazomethine (PPDA) was prepared by solution polycondensation of paraphenylene diamine and glyoxal trimeric hydrate in DMF at a molar ratio of 1:1 at 120°C for 5 h. PPDA was doped with 1 M solution of HCl for 24 h.

2.2. Testing of Polymers

DC conductivity of the pelletized samples was evaluated using Kiethley Nanovoltmeter model-614. The specific resistivity was calculated as $\rho = (R \times A)/t$, where, ρ is the resistivity, R is the resistance measured, A is the area of the electrode used, and t is the thickness of the sample. And, $\sigma = 1/\rho$, where σ is the conductivity of the material. The microwave properties of the polymers in the powder form in S band (2–4 GHz) were evaluated by cavity perturbation technique. The transmission-type resonator used in this experiment was excited with TE_{10P} mode by connecting it to an HP8510 C Network Analyzer. The dielectric parameters of the sample were evaluated from the resonant frequency and the quality factor of the empty cavity resonator and the loaded cavity. The resonant frequency f_0 and the corresponding quality factor Q_0 of each resonant peak of the empty cavity were first determined. Now after selecting a particular resonant frequency, the dielectric sample was introduced into the cavity, and the position was adjusted for maximum perturbation, and the corresponding change in the frequency of the resonant peak was observed. The new resonant frequency f_s , the corresponding 3 dB bandwidth and the quality factor Q_s were determined. The microwave properties were calculated using the equations [14, 15] given below (1–7) where ϵ_r' is the dielectric constant ϵ_r'' is the loss factor, ϵ_0 is the permittivity of free space, α_f is the absorption coefficient, δ_f is the penetration depth, σ_e is the conductivity, J is the heating coefficient, c is the velocity of light, V_c is the volume of the cavity, and V_s is the volume of the sample.

$$\epsilon_r' = 1 + \frac{f_0 - f_s}{2f_s} \left[\frac{V_c}{V_s} \right] \quad (1)$$

$$\epsilon_r'' = \frac{V_c}{4V_s} \left[\frac{Q_0 - Q_s}{Q_0 Q_s} \right] \quad (2)$$

$$J = \frac{1}{\epsilon_r \tan \delta} \quad (3)$$

$$\alpha_f = \frac{\epsilon_r'' f}{nc} \quad (4)$$

$$\sigma_e = 2\pi f \epsilon_0 \epsilon_r'' \quad (5)$$

$$\tan \delta = \frac{\epsilon_r''}{\epsilon_r'} \quad (6)$$

$$\delta_f = \frac{1}{\alpha_f} \quad (7)$$

3. RESULTS AND DISCUSSION

3.1. Microwave Properties

Dielectric Constant (ϵ_r')

The dielectric constant of different conducting polymers at S band frequency was compared in Figure 1. Figure shows that dielectric constant decreases with increase in frequency. This is due to the orientation polarization in the microwave field. The polarization is caused by the alternating accumulation of charges at interfaces between different phases of the material. This dipole polarization may be related to the "frictional" losses caused by the rotational displacement of molecular dipoles under the influence of the alternating electrical field. As the frequency of the applied field is increased, the polarization has no time to reach its steady field value and the orientation polarization is the first that falls. Because of the orientation polarization of the dipoles, the possibility of dielectric relaxation (so also dielectric loss) cannot be ruled out at higher frequencies. This might result in the decrease of ϵ_r' with frequency [16-17]. It was also clear from the figure that the dielectric constant was highest for PEDOT, and lowest for PPDA.

In conducting polymers conductivity is not constant along the conducting paths and that several relaxation times may coexist. The distribution of conductivity leads to a dispersion of ϵ' and σ without any polarization phenomenon. So, the large dielectric constants measured at low frequency in conducting polymers may also be linked to the heterogeneity of materials in the form of a conductivity variation along the conducting path. At low frequencies, the different polarizations (electronic, atomic, and dipolar polarizations) contribute to a high permittivity ϵ' value, beyond that each kind of polarization will create one resonance or one relaxation process and ϵ' decreases.

3.2. Dielectric Loss (ϵ_r'')

The dielectric loss of different conducting polymers at S band frequency was compared in Figure 2. The reorientation of the unassociated groups, because of their high dipole moment, is believed to be a major contributor to the dielectric loss (ϵ_r''). At higher frequency, the rotatory motion of the molecules may not be

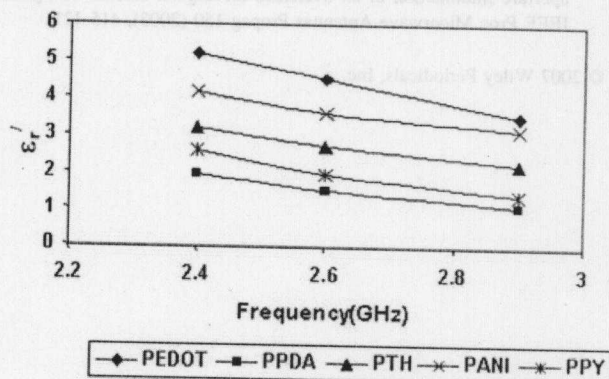


Figure 1 Variation of dielectric constant with frequency for various conducting polymers. PEDOT, PPDA, PTH, PANI, and PPY

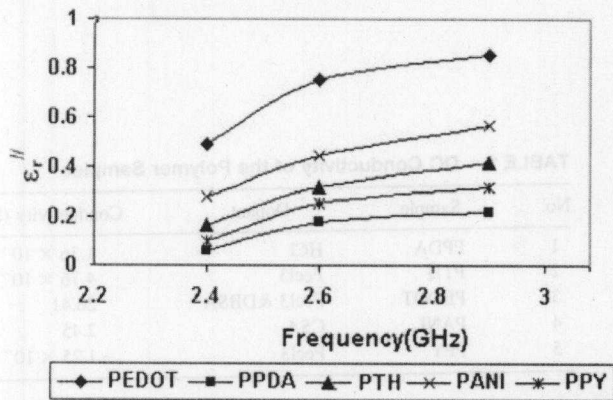


Figure 2 Variation of dielectric loss with frequency for various conducting polymers. PEDOT, PPDA, PTH, PANI, and PPY

sufficiently rapid for the attainment of equilibrium with the field. The polarization then acquires a component out of phase with the field, and the displacement current acquires a conductance component in phase with the field, resulting in thermal dissipation of energy. When this occurs, dielectric losses will be generated. Dielectric loss tends to increase with increase in frequency range 2.4–2.9 GHz. As the frequency is increased, the inertia of the molecule and the binding forces become dominant, and it is the basis for high-dielectric loss at higher frequencies. The dielectric loss factor leads to so-called conductivity relaxation. From Figure 2, it was clear that the conductivity of the polymers follow the order PEDOT > PANI > PTH > PPY > PPDA. The contributions of conduction and polarization mechanisms on dielectric loss can be separated $\epsilon'' = \epsilon''_{\text{conduction}} + \epsilon''_{\text{polarization}}$. The value of ϵ'' polarization is related to the molecular polarization phenomena such as dipole rotation (Debye model), space charge relaxation (Maxwell-Wagner model), and hopping of confined charges. The physical origin of this polarization term is often ambiguous [18, 19].

3.2.1. Loss Tangent ($\tan \delta$)

The $\tan \delta$ is commonly employed as a direct measure of the dielectric loss, which in turn provides a measure of the conductivity. Angle δ is the angle between the vector for the amplitude of the total current and that for the amplitude of charging current, and the tangent of this angle is the loss tangent [20]. Because it is

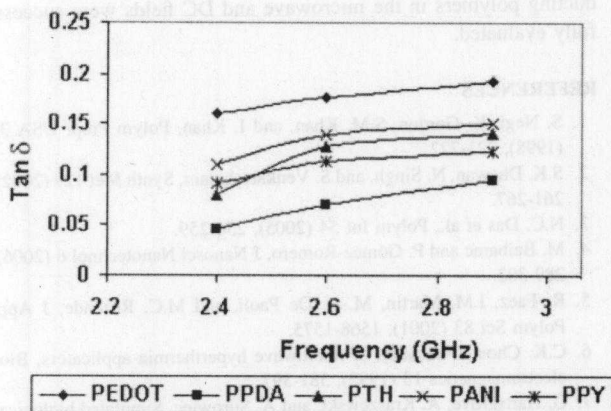


Figure 3 Variation of loss tangent with frequency for various conducting polymers. PEDOT, PPDA, PTH, PANI, and PPY

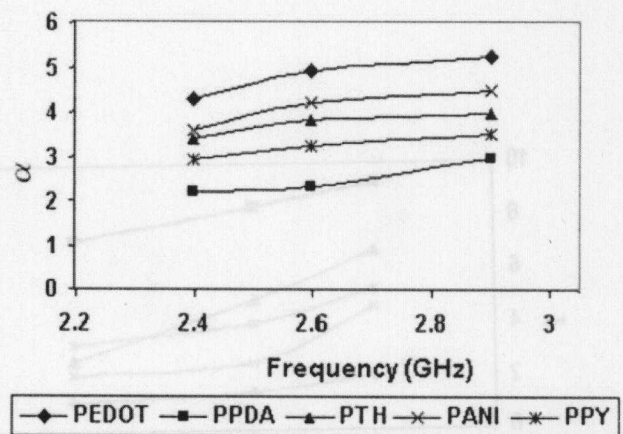


Figure 4 Variation of absorption coefficient with frequency for various conducting polymers. PEDOT, PPDA, PTH, PANI, and PPY

directly related to the dielectric loss, it shows the same behavior as that of dielectric loss. Figure 3 shows that the loss tangent of conducting polymers increases with the increase in frequency.

3.2.1. Absorption Coefficient (α)

Materials can be classified in terms of their transparency of wave passing through it, which in turn specify the absorption of electromagnetic waves when it passes through the medium [21]. The transparency is defined by the parameter, absorption coefficient. Absorption coefficient is directly related to the dielectric loss factor, and therefore it shows the same behavior as dielectric loss. Figure 4 shows that PEDOT shows highest absorption coefficient followed by PANI, PTH, PPY, and PPDA.

3.2.2. Conductivity (σ)

The microwave conductivity is a direct function of dielectric loss, and so it shows a similar variation with frequency as the dielectric loss factor. Figure 5 shows that conductivity increases with frequency. Here, also the trend continues with PEDOT showing the best conductivity followed by PANI, PTH, PPY, and PPDA successively.

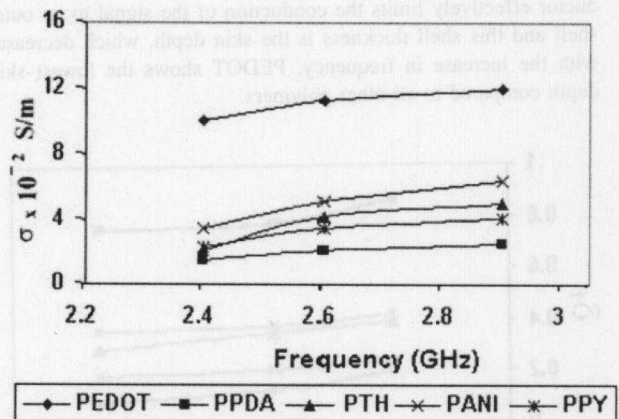


Figure 5 Variation of conductivity with frequency for various conducting polymers. PEDOT, PPDA, PTH, PANI, and PPY

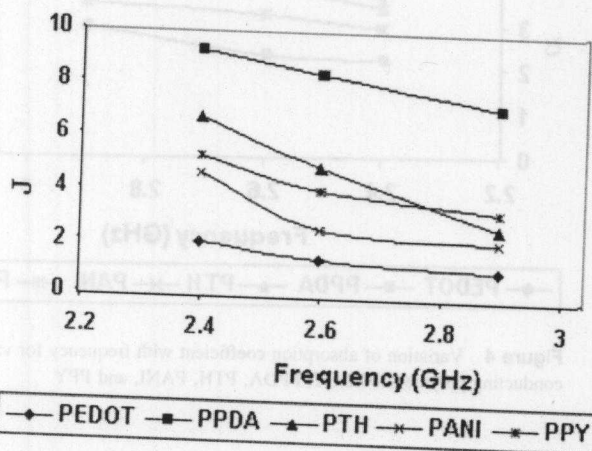


Figure 6 Variation of heating coefficient with frequency for various conducting polymers. PEDOT, PPDA, PTH, PANI, and PPY

3.2.3. Dielectric Heating Coefficient (J)

As the heat generation in polymers is due to relaxation loss, the efficiency of heating of a polymer is compared by means of a heating coefficient [22] J . Higher the J value, poorer will be the polymer for dielectric heating purposes. Of course, the heat generated in the polymeric material comes from the loss tangent, but that loss may not come entirely from the relaxation loss. Rather, conductivity of the polymeric material may also contribute to the $\tan \delta$. This situation may be compared with ohmic heating of metals [17]. The heating coefficient is inversely related to the loss tangent, and hence it decreases with increase in frequency. It was clear from the Figure 6 that PEDOT was an efficient material for heating applications because it shows minimum heating coefficient. It was also clear that heating coefficient follows the order PEDOT < PANI < PPY < PTH < PPDA.

3.2.4. Skin Depth (δ_s)

Figure 7 shows that skin depth decreases with the increase in frequency. It is the effective distance of penetration of an electromagnetic wave into the material. It can be applied to a conductor carrying high-frequency signals. The self inductance of the conductor effectively limits the conduction of the signal to its outer shell and this shell thickness is the skin depth, which decreases with the increase in frequency. PEDOT shows the lowest skin depth compared to all other polymers.

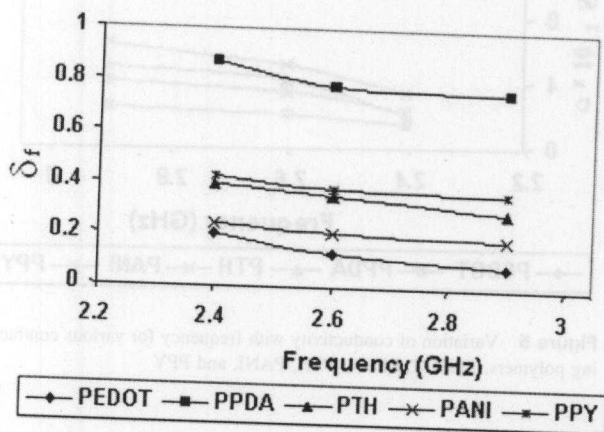


Figure 7 Variation of skin depth with frequency for various conducting polymers. PEDOT, PPDA, PTH, PANI, and PPY

TABLE 1 DC Conductivity of the Polymer Samples

No.	Sample	Dopant	Conductivity (S/m)
1	PPDA	HCl	1.36×10^{-4}
2	PTH	FeCl ₃	4.76×10^{-1}
3	PEDOT	FeCl ₃ & DBSA	26.41
4	PANI	CSA	2.45
5	PPY	FeCl ₃	1.25×10^{-1}

3.2. DC Conductivity

DC conductivity of the polymer samples are shown in Table 1. The DC conductivity of PEDOT was found to be very high compared to all other conducting polymers and the conductivity follows the order PEDOT > PANI > PTH > PPY > PPDA. PANI and PEDOT are reported to show very good DC conductivity. In the case of PEDOT synthesized in DBSA micellar solutions, DBSA-FeCl₃ complex is expected to be formed. The anchoring efficiency of dodecylbenzene sulfonate anion with iron (III) on the PEDOT particles seems to increase the doping of the bulky anionic surfactant and gives good conductivity [11].

4. CONCLUSIONS

Dielectric constant, dielectric loss, conductivity, absorption coefficient, heating coefficient, loss tangent, and skin depth of conducting polymers such as PEDOT, PTH, PANI, and PPDA are studied and compared at S band frequency. It was found that dielectric constant, dielectric loss, $\tan \delta$, conductivity, and absorption coefficient of the conducting polymers show a trend in the order PEDOT > PANI > PTH > PPY > PPDA. But heating coefficient and skin depth of the conducting polymers show a trend in the reverse order PEDOT < PANI < PTH < PPY < PPDA. Comparing the different polymers, better microwave properties are shown by PEDOT and PANI. Dielectric constant, heating coefficient, and skin depth tend to decrease with the increase in frequency, and dielectric loss, conductivity, loss tangent, and absorption coefficient increases with frequency in S band. DC conductivity of the conducting polymers also show a similar trend as in the case of AC conductivity PEDOT > PANI > PTH > PPY > PPDA. The dielectric properties of some important conducting polymers in the microwave and DC fields were successfully evaluated.

REFERENCES

1. S. Negi, K. Gordon, S.M. Khan, and I. Khan, Polym Prepr USA 39 (1998), 721-722.
2. S.K. Dhawan, N. Singh, and S. Venkatachalam, Synth Met 129 (2002), 261-267.
3. N.C. Das et al., Polym Int 54 (2005), 256-259.
4. M. Baibarac and P. Gómez-Romero, J Nanosci Nanotechnol 6 (2006), 289-302.
5. R. Faez, I.M. Martin, M.-A. De Paoli, and M.C. Rezende, J Appl Polym Sci 83 (2001), 1568-1575.
6. C.K. Chou, Evaluation of microwave hyperthermia applicators, Bioelectromagnetics 13 (1992), 581-597.
7. G. Hartsgrove, A. Kraszewski, and A. Surowiec, Simulated biological materials for electromagnetic radiation absorption studies, Bioelectromagnetics 8 (1987), 29-36.
8. J.T. Chang, M.W. Fanning, P.M. Meaney, and K.D. Paulsen, IEEE Trans Electromagn Compat 42 (2000).
9. D. Andreuccetti, M. Bini, A. Ignesti, R. Olmi, N. Rubino, and R. Vanni, Use of polyacrylamide as a tissue-equivalent material in the microwave range, IEEE Trans Biomed Eng 35 (1988), 275-277.
10. T. Yamamoto et al., Macromolecules 25 (1992), 1214.
11. J.W. Choi et al., Synth Met 141 (2004), 293-299.

12. Subramaniam, Radhakrishnan, Deshpande, and S. Dagadopant, U. S. Pat. 0,198,948 (2004).
13. S. Machida, S. Miyata, and A. Techagumpuch, Synth Met 31 (1989) 31.
14. K.T. Mathew and U. Raveendranath, Sensors Update, 7 (1999), 185.
15. K.T. Mathew et al., Mater Chem Phys 79 (2003), 187-190.
16. E.J. Frommer and R.R. Chance, Electrical and electronic properties of polymers: A state-of-the-art compendium, encyclopedia reprint series, In: I.J. Kroschwitz (Ed.), Wiley/Interscience, New York, 1988, pp. 101-178.
17. T.A. Ezquerro, F. Kremmer, and G. Wegner, AC electrical properties of insulator conductor composites, In: A. Priou (Ed.), Dielectric properties of heterogeneous materials: Progress in electromagnetic research, Vol. 6, Elsevier, New York, 1992.
18. Legros and A. Fourier-Lamer, Mater Res Bull 19 (1984), 1109.
19. A. Moliton, J.L. Duroux, and G. Froyer, Ann Phys Fr (1988) 261-287.
20. L. Olmedo et al., Revue Compos Nouveaux Mater 1 (1991), 123.
21. C.K. Chen and R. Liepins, Electrical properties of polymers: Chemical principles, Hanser, Munich, 1987.
22. I.S. Bradford and M.H. Carpentier, The microwave engineering handbook, Chapman & Hall, London, 1993.

© 2007 Wiley Periodicals, Inc.

ASYMMETRIC LONG AND THICK DIPOLES FOR IN-FLIGHT TELEMETRY OF PROJECTILES

L. Bernard

French-German Research Institute of Saint Louis, 5, rue du Général Cassagnou, BP 70034, 68301 Saint Louis France; Corresponding author: bernard@isl.tm.fr

Received 28 June 2007

ABSTRACT: Long and thick dipoles are presented, with a feeding point located off the centre. Parameter studies are performed, showing that asymmetric radiation patterns with a main lobe in a preferred direction can be achieved. Experimental results confirm the feasibility of these antennas and illustrate possible applications. © 2007 Wiley Periodicals, Inc. Microwave Opt Technol Lett 50: 508–511, 2008; Published online in Wiley InterScience (www.interscience.wiley.com). DOI 10.1002/mop.23105

Key words: long dipole; feed location; coaxial feeding; telemetry

1. INTRODUCTION

Dipoles are commonly used antennas in communication systems due to their simplicity, their quite wide bandwidth, and their omnidirectional radiation pattern in the plane normal to the axis of the dipole. Many developments have been made on centre-fed dipole of negligible diameters, finite diameters, and various lengths [1–3]. The thick dipoles have a wider bandwidth than the thin ones and the radiation pattern of dipoles longer than a wavelength presents more than two lobes (the number of lobes increases with the length) [3]. As the driving point is off the dipole centre, the current distribution along the dipole becomes asymmetric and hence the radiated fields too [4]. For dipoles with a negligible diameter, the longitudinal current distribution is usually assumed to be of sinusoidal form and hence the radiation patterns can be fast calculated. When the diameter is not negligible, in particular for thick dipoles, EM codes are required to achieve accurate results.

In the area of instrumentation of projectiles for in-flight telemetry, some specific requirements for the antennas depend on the

physical dimensions of the projectile and of the test configurations. In particular the antenna integration should not modify the flight characteristics by changing the mass distribution of the projectile and so the position of its center of gravity. In this article, we propose the design of an antenna using the body itself of an instrumented projectile to constitute an asymmetric long dipole. In fact the work frequency is in the S-band and more precisely should be between 2200 and 2350 MHz (the wavelength in free space λ is about 130 mm at $f = 2300$ MHz). The caliber of the projectile is $d = 30$ mm (0.23λ at 2300 MHz) and its length $l = 300$ mm (2.3λ) [5]. Considering this last value the projectile can be considered as a long dipole and we expect to obtain a multilobe radiation pattern with a main lobe steered from the direction perpendicular to the dipole axis [3]. Moreover, the feeding of the dipole is not located at its centre but placed preferably at a given position on one branch of the dipole to obtain an asymmetric radiation pattern with a main lobe lateral and toward the back.

The characteristics of a long dipole of length $l = 2.3\lambda$ are presented in a first section. The two branches are of same length. The influence of the diameter on the radiation patterns is investigated and the possibility to use a simple model of an infinitesimally thin dipole is also treated. In a second time, the asymmetry of the dipole is used by moving the feeding position to obtain a main lobe in one preferred direction. The influence of the feed location on the impedance is investigated. The final design and measured results are presented in a third and last point. In particular, the advantages of having a thick dipole (imposed by the projectile caliber) on the bandwidth of this antenna are demonstrated.

2. SYMMETRIC LONG DIPOLE

In this section, the characteristics of a linear cylinder of diameter d and of length $l = 300$ mm are investigated at frequency $f = 2300$ MHz ($\lambda = 130$ mm). The simulations are performed with the software Ansoft HFSS [6], based on the finite-element method. The metallic cylinder is cut in two branches separated by a dielectric material at distance h from the centre (Fig. 1). The thickness of this material is $h_d = 6$ mm and its relative permittivity is $\epsilon_r = 3.5$ ($\tan \delta = 0.01$). The feeding is obtained with a 50- Ω coaxial line located inside one branch and whose inner conductor is connected to the other branch, whereas the outer connector is connected to this precise branch.

First, the influence of the thick diameter is investigated. Therefore a centre-fed dipole ($h = 0$) is simulated, which three different values of diameter $d = l/50 = 6$ mm, $d = l/10 = 30$ mm, and $d = l/5 = 60$ mm. The normalized radiation pattern of an infinitesimally

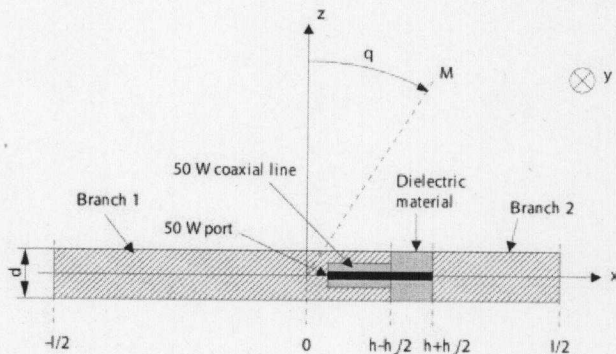


Figure 1 Description of the long asymmetric dipole